ELSEVIER

Biochimica et Biophysica Acta 1564 (2002) 173–182

BIOCHIMICA ET BIOPHYSICA ACTA
BBA

www.bba-direct.com

La^{3+} and Gd^{3+} induce shape change of giant unilamellar vesicles of phosphatidylcholine

Tomoki Tanaka [a], Yukihiro Tamba [a], Shah Md. Masum [a], Yuko Yamashita [b], Masahito Yamazaki [a,b,*]

[a] *Materials Science, Graduate School of Science and Engineering, Shizuoka University, 422-8529, Japan*
[b] *Department of Physics, Faculty of Science, Shizuoka University, Shizuoka, 422-8529, Japan*

Received 10 October 2001; received in revised form 12 February 2002; accepted 11 April 2002

Abstract

Lanthanides such as La^{3+} and Gd^{3+} are well known to have large effects on the function of membrane proteins such as mechanosensitive ionic channels and voltage-gated sodium channels, and also on the structure of phospholipid membranes. In this report, we have investigated effects of La^{3+} and Gd^{3+} on the shape of giant unilamellar vesicle (GUV) of dioleoylphosphatidylcholine (DOPC-GUV) and GUV of DOPC/cholesterol by the phase-contrast microscopy. The addition of 10–100 μM La^{3+} (or Gd^{3+}) through a 10-μm diameter micropipette near the DOPC-GUV (or DOPC/cholesterol-GUV) triggered several kinds of shape changes. We have found that a very low concentration (10 μM) of La^{3+} (or Gd^{3+}) induced a shape change of GUV such as the discocyte via stomatocyte to inside budded shape transformation, the two-spheres connected by a neck to prolate transformation, and the pearl on a string to cylinder (or tube) transformation. To understand the effect of these lanthanides on the shape of the GUV, we have also investigated phase transitions of 30 μM dipalmitoylphosphatidylcholine-multilamellar vesicle (DPPC-MLV) by the ultra-sensitive differential scanning calorimetry (DSC). The chain-melting phase transition temperature and the $L_{\beta'}$ to $P_{\beta'}$ phase transition temperature of DPPC-MLV increased with an increase in La^{3+} concentration. This result indicates that the lateral compression pressure of the membrane increases with an increase in La^{3+} concentration. Thereby, the interaction of La^{3+} (or Gd^{3+}) on the external monolayer membrane of the GUV induces a decrease in its area (A^{ex}), whereas the area of the internal monolayer membrane (A^{in}) keeps constant. Therefore, the shape changes of the GUV induced by these lanthanides can be explained reasonably by the decrease in the area difference between two monolayers ($\Delta A = A^{ex} - A^{in}$).

Keywords: Lanthanum ion; Gadolinium ion; Giant unilamellar vesicle; Shape of vesicle; Bilayer-couple model; Lateral compression pressure

1. Introduction

Lanthanum ion (La^{3+}) and gadolinium ion (Gd^{3+}), which are lanthanides, are well known to play important roles in the structure and function of biomembranes or phospholipid membrane. In the research field of ionic channel proteins, Gd^{3+} is well known as a blocker of stretch-activated ionic channels (mechanosensitive ionic channels) [1–4], and La^{3+} can modulate the gating properties of voltage-gated sodium channel [5,6]. The lanthanides also have effects on the structure and stability of phospholipid membranes. Interaction of La^{3+} with the surface of negatively charged phosphatidylserine (PS) membrane effectively induces membrane fusion of PS vesicles [7–9]. Moreover, interaction of La^{3+} with the head groups of electrical-neutral phosphatidylcholine (PC) membrane moves the N end of P → N vector of the head groups toward the water phase [10–12]. However, the effects of the interaction of the lanthanides with the membrane interface on stability of membrane structure and functions of membrane proteins are not well understood.

Giant unilamellar vesicles (GUVs) of phospholipids, with diameters in the range of 10–100 μm, can be used to investigate elastic properties of the phospholipid membranes [13–15] and shape change of vesicles [16–21]. These studies have been considered helpful to understand dynamics of biological membranes such as various structures of membranes in the cell, endocytosis, and membrane fusions.

Abbreviations: GUV, giant unilamellar vesicle; MLV, multilamellar vesicle; DOPC, 1,2-dioleoyl-*sn*-glycero-3-phosphatidylcholine; L_α phase, liquid-crystalline phase; $L_{\beta'}$ phase, bilayer gel phase with tilted hydrocarbon chains; $P_{\beta'}$ phase, ripple phase

* Corresponding author. Department of Physics, Faculty of Science, Shizuoka University, 836 Oya, Shizuoka 422-8529, Japan. Tel./fax: +81-54-238-4741.

E-mail address: spmyama@ipc.shizuoka.ac.jp (M. Yamazaki).

0005-2736/02/$ - see front matter
PII: S0005-2736(02)00444-3

In theoretical investigations, there are two approaches based on the assumption that the shape of GUV at equilibrium is determined by the minimization condition of membrane bending energy [22–24]. Deuling and Helflich [22] described the shape change by the spontaneous-curvature model. In this model, the shape of GUV is determined by the minimum bending energy for a given area A and a given volume V. On the other hand, Svetina and Zeks [23], and also Seifert et al. [24] have proposed a bilayer-couple model; in this model, the shape of GUV is determined by the minimum bending energy for a given area A, a given volume V, and also a given area difference between the two monolayers in the bilayer membrane ΔA. Recently, the area-difference-elasticity (ADE) model has been proposed to generalize the bilayer-couple model, where the effect of the elastic energy due to the stretching of the monolayer membrane is included [25–27]. On the other hand, in the experimental approach, Sackmann et al. [17,18] have investigated temperature dependence of the shape of GUV of dimyristoylphosphatidylcholine (DMPC). Assuming that there is a small difference in the thermal expansivities of the two monolayers, the bilayer-couple model can explain the shape change of the GUV induced by the temperature change reasonably. Devaux et al. [19,28] found that the redistribution of less than 1% of the total phospholipid was sufficient to induce the shape change in GUV, which can be explained by the bilayer-couple model.

In this report, we have investigated the effects of La^{3+} (or Gd^{3+}) on the shape of GUV of dioleoylphosphatidylcholine (DOPC-GUV) by the phase-contrast microscopy. We have found a very low concentration (10 μM) of La^{3+} (or Gd^{3+}) induced several kinds of shape changes of GUV. Major ones are a discocyte (i.e., biconcave disc shape) via stomatocyte (i.e., cupped form) to inside budded shape transformation, a two-spheres connected by a neck to prolate transformation, and a pearl on a string (i.e., several spherical vesicles connected by a narrow tube) to cylinder (or tube) transformation. To understand the effects of these lanthanides on the phosphatidylcholine (PC) membranes, we also investigated phase transitions of a low concentration (30 μM) of dipalmitoylphosphatidylcholine-multilamellar vesicle (DPPC-MLV) by the ultra-sensitive differential scanning calorimetry (DSC). This concentration of the DPPC-MLV is almost the same as that of the DOPC-GUV used in the experiment of the shape change. The chain-melting phase transition temperature and the $L_{\beta'}$ to $P_{\beta'}$ phase transition (pre-transition) temperature of DPPC-MLV also increased with an increase in La^{3+} concentration. This result indicates that the lateral compression pressure of the membrane increases with an increase in La^{3+} concentration. Moreover, effect of La^{3+} on the spontaneous curvature of DOPC/cholesterol monolayer membrane was investigated using a small-angle X-ray scattering (SAXS), which indicates that La^{3+} induces a decrease in the surface area of this membrane. Based on these results, we discuss the mechanism of the La^{3+} (or Gd^{3+})-induced shape change of DOPC-GUV.

2. Materials and methods

2.1. Materials and sample preparation

1,2-dioleoyl-*sn*-glycero-3-phosphatidylcholine (DOPC) and 1,2-dipalmitoyl-*sn*-glycero-3-phosphatidylcholine (DPPC) were purchased from Avanti Polar Lipids $LaCl_3$ ($\geq$99.9%), $GdCl_3$ ($\geq$99.9%), and cholesterol were purchased from Wako Chemical Co. 2-[12-(7-nitrobenz-2-oxa-1, 3-diazol-4-yl) amino] dodecanoyl-1-hexadecanoyl-*sn*-glycero-3-phosphocholine (NBD-PC) was purchased from Molecular Probes Inc.

2.2. Formation of GUV

GUVs of phospholipid were prepared as follows: 100 μl of 1 mM phospholipid (DOPC or DOPC/cholesterol mixture) in chloroform in a small glass vessel was dried by N_2 gas, and then the solvent was completely removed by placing the sample in a vacuum desiccator connected to a rotary vacuum pump for more than 12 h. Ten microliters of water was added into this vessel, and it was incubated at 45 °C for a few minutes (pre-hydration). Then, 3 ml of 0.1 M sucrose in water was added, and incubated at 37 °C for 2 h.

2.3. Observation of GUVs under a phase-contrast microscope and a fluorescent microscope

Ten microliters of GUV solution (0.1 M sucrose solution; internal solution) was diluted into 290 μl of 0.1 M glucose aqueous solution (external solution), and then injected into a hand-made microchamber. This chamber (1 × 1 cm wide and 3 mm high, internal volume is ~ 0.3 ml) was formed on a slide glass by inserting a U-shaped silicone-rubber spacer between a cover glass and the slide glass. We observed GUVs by an inverted phase-contrast microscope (IX-70, Olympus, Tokyo, Japan) at 20 ± 2 °C. Phase-contrast images of GUVs were recorded through a charge-coupled-device (CCD) camera (DXC-108, SONY) on a video recorder.

As GUVs, we selected the vesicles of which the contrast of the membrane was very low and undulation motion of the membrane was large. When we observed these vesicles containing a small percentage (0.5 mol%) of long-chain fluorescent phospholipid, NBD-PC, by the fluorescence microscope (IX-70, Olympus), the intensities of fluorescence from these vesicles were much lower than those from multilamellar vesicles.

2.4. Shape change of GUV

Various kinds of concentrations of La^{3+} (or Gd^{3+}) in 0.1 M glucose aqueous solution were added into the neighborhood of a GUV through a 10-μm diameter glass micropipette, whose position was controlled by a micromanipulator (MMW-23, Narishige, Tokyo, Japan). For this purpose, we used a hand-made apparatus for the micropipette aspira-

tion method [13] to measure the isothermal area compressibility modulus of the membrane of GUV. The glass micropipette was pulled from 1.0 mm glass tubing (G-1, Narishige) to a needlepoint by a puller (PP-83, Narishige), and then broken by quick fracture to the desired tip diameter. The micropipette filled with 0.1 M glucose aqueous solution containing several kinds of concentrations of La^{3+} (or Gd^{3+}) by aspiration using a vacuum pump. We controlled the injection pressure by changing the height of vertical column of water in a U-shaped glass tube to which the micropipette was hydraulically connected.

2.5. Ultra-sensitive DSC

The microcalorimeter (VP-DSC, Microcal Inc., Northampton, USA) was used. We set the feedback mode high, and the filtering period at 5 s. DPPC-MLV dispersion in water containing various kinds of concentrations of La^{3+} (for the raw sample data) and the same aqueous solution without DPPC-MLV (for the reference data) were heated at a rate of 1.0 K/min from 20 to 60 °C. The genuine sample data was obtained by subtracting the reference data from the raw sample data. Under these conditions, the noise level of the DSC curve was in the range of 2–3 μcal/°C. Phase transition temperatures were determined by the peak of the endothermic curve.

DPPC-MLV was prepared by adding appropriate amounts of water or 0.5 M KCl aqueous solution containing various kinds of concentrations of La^{3+} to the dry lipids in excess water condition, and the suspension was vortexed for 30 s several times at around 50 °C. The concentration of phospholipid in the sample for the measurement of the DSC was determined by the standard phosphate analysis [29].

2.6. X-ray diffraction

X-ray diffraction experiments were performed by using Nickel filtered Cu K_α X-ray ($\lambda = 0.154$ nm) from rotating anode type X-ray generator (40 kV × 200 mA) (Rotaflex, RU-300, Rigaku, Tokyo, Japan). SAXS data were recorded using a linear (one-dimensional) position sensitive proportional counter (PSPC-5, Rigaku) with a camera length of 350 mm and analyzed by the multichannel analyzer (Rigaku) and the computer. Samples were sealed in a thin-walled glass capillary tube (outer diameter, 1.0 mm) and mounted in a thermostable holder whose stability was ± 0.2 °C [30].

We investigated spontaneous curvature of 60 mol% DOPC/40 mol% cholesterol monolayer membrane containing 16 wt.% tetradecane (Fig. 7) as follows [31,32]. The appropriate amount of DOPC and cholesterol mixture in chloroform was dried by N_2 gas, and then under vacuum by rotary pump for more than 12 h. Tetradecane was added to the dry lipid by weighing directly. After 24 h incubation at room temperature (~ 25 °C) for equilibration, the appropriate amount of a given concentration of La^{3+} in 10 mM PIPES buffer (pH 7.0) was added to this dry-lipids/tetradecane mixture in excess solvents (~ 7 wt.% lipids), and the suspension was vortexed for 30 s at room temperature (~ 25 °C) several times, and then incubated for another 48 h for equilibration. For measurement of X-ray diffraction, pellets of the suspensions after centrifugation (13,000 × *g*, 30 min at 20 °C) (MR-150, Tomy, Tokyo, Japan) were used.

3. Results

3.1. Shape changes of GUV induced by La^{3+} and Gd^{3+}

Fig. 1a shows a shape change of a DOPC-GUV induced by addition of 100 μM $LaCl_3$ through a 10-μm diameter micropipette near the GUV. At first (in the absence of La^{3+}),

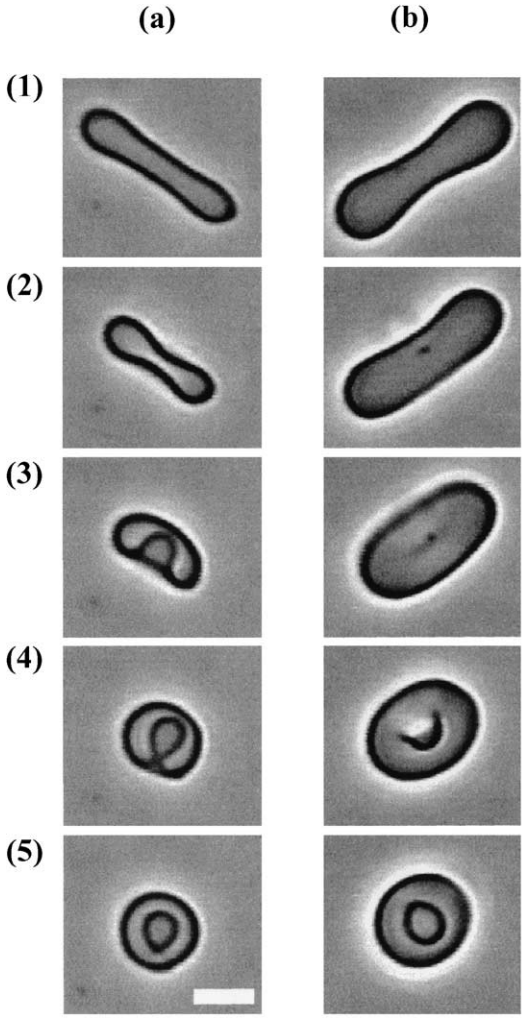

Fig. 1. Shape change of DOPC-GUV induced by the addition of (a) 100 μM La^{3+} and (b) 10 μM Gd^{3+} at 20 °C. The discocyte via stomatocyte to inside budded shape transition occurred. The time after starting injection of La^{3+} (or Gd^{3+}) solution through the micropipette is (1) 0 s, (2) 2 s, (3) 4 s, (4) 6 s, and (5) 12 s for the pictures of (a), and (1) 0 s, (2) 3 s, (3) 4 s, (4) 6 s, and (5) 7 s for the pictures of (b). The bar in the picture corresponds to 10 μm.

the GUV was a discocyte. After the addition of La^{3+}, the shape changed into the stomatocyte (Fig. 1a, (3)). Further addition of La^{3+}, the stomatocyte invagination became unstable and a small vesicle budded into the inside of the GUV (Fig. 1a, (5)). We observed this shape change in 14 GUVs among 14 examined GUVs ($n=14$). When 10 μM La^{3+} was added to the neighborhood of a GUV instead of 100 μM La^{3+} in this experiment, a similar shape change (the discocyte via stomatocyte to inside budded shape transition) was observed in 46 GUVs among 46 examined GUVs ($n=46$). When 1 μM La^{3+} was added near the GUV for 5 min, this type of shape change was not observed. We can call this shape change the discocyte via stomatocyte to inside budded shape transformation. As a control experiment, 1 mM NaCl was added near the GUV for 15 min, but no shape change of the GUV was observed.

Fig. 2 shows another type of shape change of DOPC-GUV induced by the addition of 10 μM La^{3+}. When we added 10 μM La^{3+} near a two-spheres connected by a neck (Fig. 2a, (1)), the shape of the GUV changed into the prolate (Fig. 2a, (3)). We observed this shape change such as Fig. 2a in 10 GUVs among 10 examined GUVs ($n=10$). When we added 10 μM La^{3+} near GUVs made of three or a series of many spherical vesicles connected by a narrow tube (so-called "pearl on a string") (Fig. 2b, (1), c, (1)), their shapes changed into a cylinder (or tube) (Fig. 2b, (3), c, (3)). We observed this shape change such as Fig. 2b and c in 20 GUVs among 20 examined GUVs ($n=20$). When 1 μM La^{3+} was added near the GUV for 5 min instead of 10 μM La^{3+} in this experiment, this type of shape change was not observed. We can call this shape change the two-spheres connected by a neck to prolate transformation (Fig. 2a) and the pearl on a string to cylinder (or tube) transformation (Fig. 2b,c).

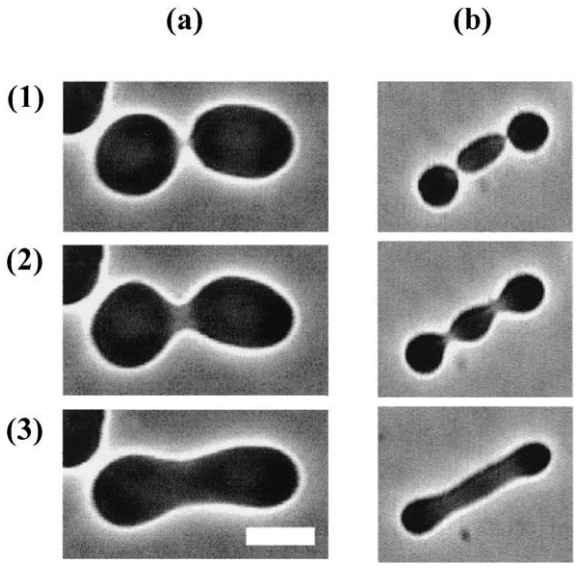

Fig. 2. Shape change of DOPC-GUV induced by the addition of 10 μM La^{3+} at 20 °C. The two-spheres connected by a neck to prolate transformation (a) and the pearl on a string to cylinder (or tube) transformation ((b) and (c)) occur. The time after starting injection of La^{3+} solution through the micropipette is (1) 0 s, (2) 2 s, and (3) 7 s for the pictures of (a), and (1) 0 s, (2) 10 s, and (3) 19 s for the pictures of (b), and (1) 0 s, (2) 5 s, and (3) 8 s for the pictures of (c). The bar in the picture (a) and (b) corresponds to 10 μm, and the bar in the picture (c) corresponds to 20 μm.

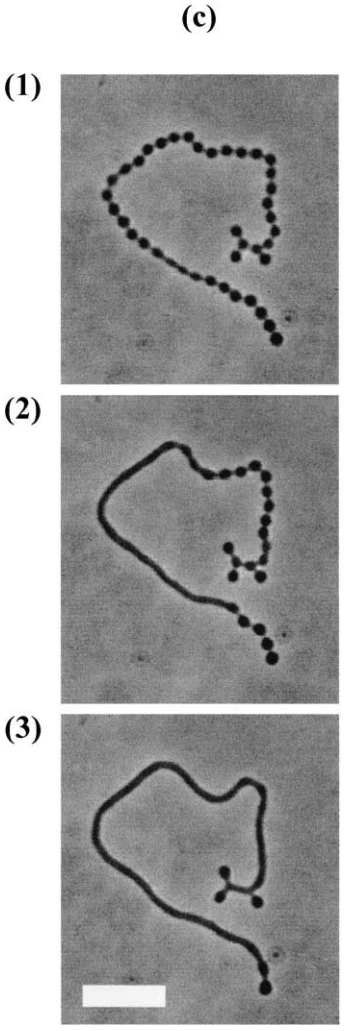

Fig. 2 (*continued*).

When 100 μM La^{3+} was added near a spherical GUV, at first, the undulation motion of the membrane of the GUV decreased, and finally, the GUV suddenly burst. We observed this shape change in 20 GUVs among 20 examined GUVs ($n=20$). When 10 μM La^{3+} was added near the GUV for 5 min instead of 100 μM La^{3+}, spherical GUVs did not burst.

Gd^{3+} had a similar effect on the DOPC-GUV as La^{3+}. The shape change from the discocyte via stomatocyte to inside budded shape ($n=11$) (Fig. 1b) and the shape change from the pearl on a string to a cylinder ($n=6$) (data not shown) was observed by addition of 10 μM Gd^{3+}. When 1 μM Gd^{3+} was added near the GUV for 5 min, these types of shape changes were not observed.

In order to determine the reversibility of the shape change induced by La^{3+}, the addition of these ions through

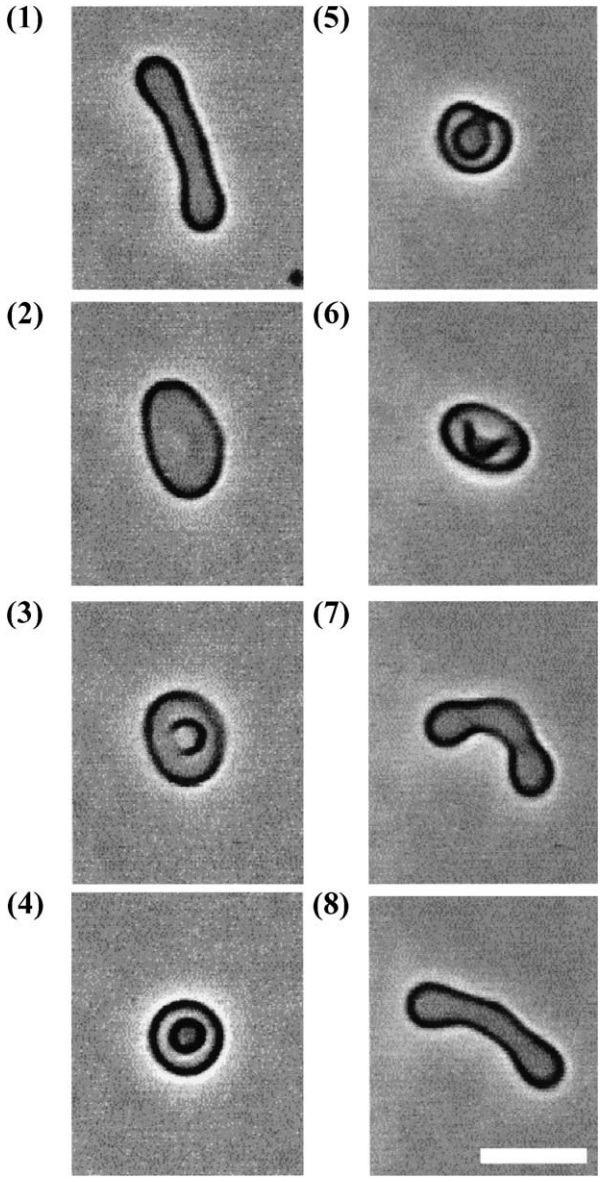

Fig. 3. The reversibility of the shape change of DOPC-GUV induced by the addition of 10 μM La^{3+} at 20 °C. During the addition of La^{3+}, the discocyte via stomatocyte to inside budded shape transition occurred. The time after starting injection of La^{3+} solution through the micropipette is (1) 0 s, (2) 9 s, (3) 10 s, and (4) 12 s for the pictures. After the addition of La^{3+} was stopped, the shape change was reversed. The time after stopping injection of La^{3+} solution through the micropipette is (5) 7 s, (6) 12 s, (7) 22 s, and (8) 33 s for the pictures. The bar in the picture corresponds to 20 μm.

the micropipette was stopped after the shape change of the GUV (the discocyte via stomatocyte to inside budded shape transformation) completed. Fig. 3 ((4)–(8)) shows the time course of the shape change of the GUV during the stop of the addition of 10 μM La^{3+}; the inside budded shape became the stomatocyte, and then changed into the discocyte. In this experiment, 10 μM La^{3+} was added to the vicinity of the GUV through the micropipette, and thereby, during the stop of the addition, La^{3+} diffused away from the vicinity of the GUV, inducing the decrease in La^{3+} concentration near the GUV. Therefore, the result of Fig. 3 indicates that the shape change induced by La^{3+} was reversible, indicating that no vesicle fission occurred. We observed the reversibility of this shape change in 35 GUVs among 36 examined GUVs ($n=36$). The other shape changes of the GUV from the two-spheres connected by a neck to prolate transformation and from the pearl on a string to cylinder transformation induced by La^{3+} were also reversible. Similar results were obtained in the shape change of the GUVs induced by Gd^{3+}, indicating that the Gd^{3+}-induced shape change of DOPC-GUVs were reversible.

It is well known that the increase in content of cholesterol in phospholipid membranes induces an increase in the area expansibility modulus [33]. The addition of cholesterol into the DOPC membrane in the GUV up to 40 mol% did not change the effects of La^{3+} (or Gd^{3+}) on the shape of the GUV; i.e., the discocyte via stomatocyte to inside budded shape transformation, the two-spheres connected by a neck to prolate transformation, and the pearl on a string to cylinder transformation were observed by addition of 10 μM La^{3+} (or Gd^{3+}). The shape change of the GUVs was reversible, indicating that no vesicle fission occurred. We observed the reversibility of this shape change in 45 GUVs among 47 examined GUVs ($n=47$).

3.2. Effect of La^{3+} on phase transition temperatures of DPPC-MLV

We have investigated the dependence of the phase transition temperatures of DPPC-MLV in water on La^{3+} concentration using the ultra-sensitive DSC. Fig. 4 shows DSC heating curves of 30 μM DPPC-MLV in water (0 mM

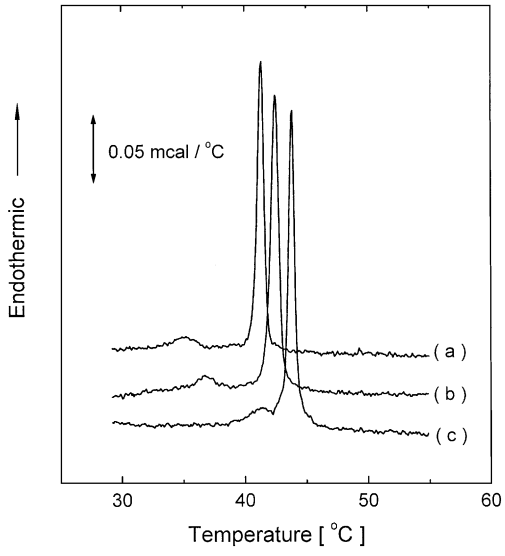

Fig. 4. DSC heating curves of 30 μM DPPC-MLV in various La^{3+} concentrations: (curve a) 0 mM, (curve b) 5 mM, (curve c) 50 mM La^{3+}. Heating rate was 1.0 °C/min.

KCl) in the presence of various concentrations of La^{3+}. As shown in Fig. 5, the chain-melting phase transition temperature (T_m) of 30 μM DPPC-MLV in 0 M KCl aqueous solution increased with an increase in La^{3+} concentration. The $L_{\beta'}$ to $P_{\beta'}$ phase transition temperature of 30 μM DPPC-MLV also increased with an increase in La^{3+} concentration. The dependence of these phase transition temperatures of 5.0 mM DPPC-MLV was almost the same as that of 30 μM DPPC-MLV (Fig. 5b). On the other hand, in the presence of 0.5 M KCl, the increments of the chain-melting temperature of 30 μM DPPC-MLV at the same La^{3+} concentrations were larger than those in the absence of KCl (Fig. 6).

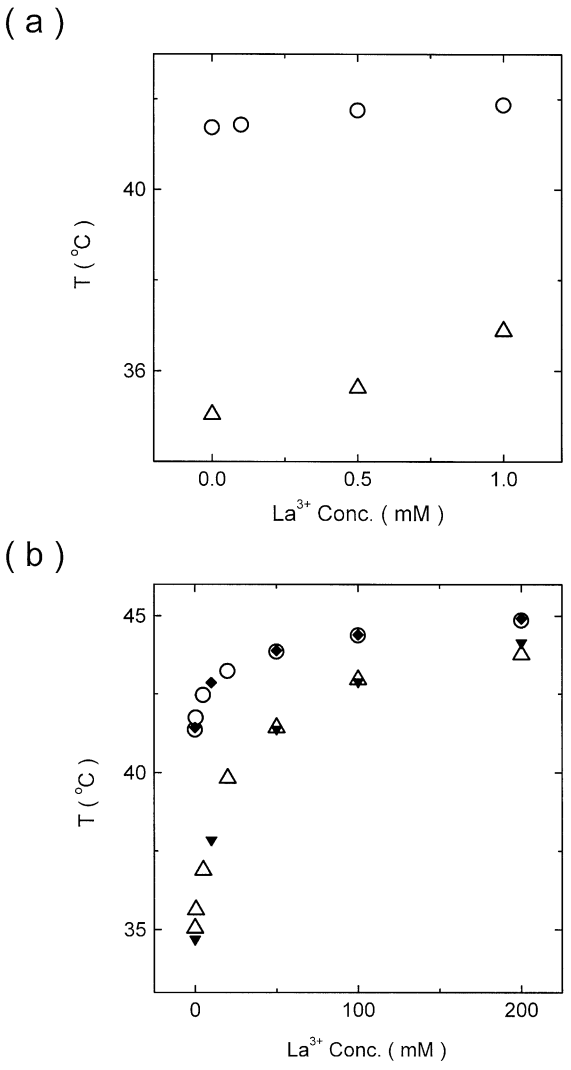

Fig. 5. Dependence of phase transition temperatures of DPPC-MLV on La^{3+} concentration. (a) 0–1 mM La^{3+} concentration range. Chain-melting transition temperature (○) and the $L_{\beta'}$ to $P_{\beta'}$ phase transition temperature (△) of 30 μM DPPC-MLV; (b) 0–200 mM La^{3+} concentration range. Chain-melting transition temperature of 30 μM DPPC-MLV (○) and of 5.0 mM DPPC-MLV (◆), and the $L_{\beta'}$ to $P_{\beta'}$ phase transition temperature of 30 μM DPPC-MLV (△) and of 5.0 mM DPPC-MLV (▼). Heating rate was 1.0 °C/min.

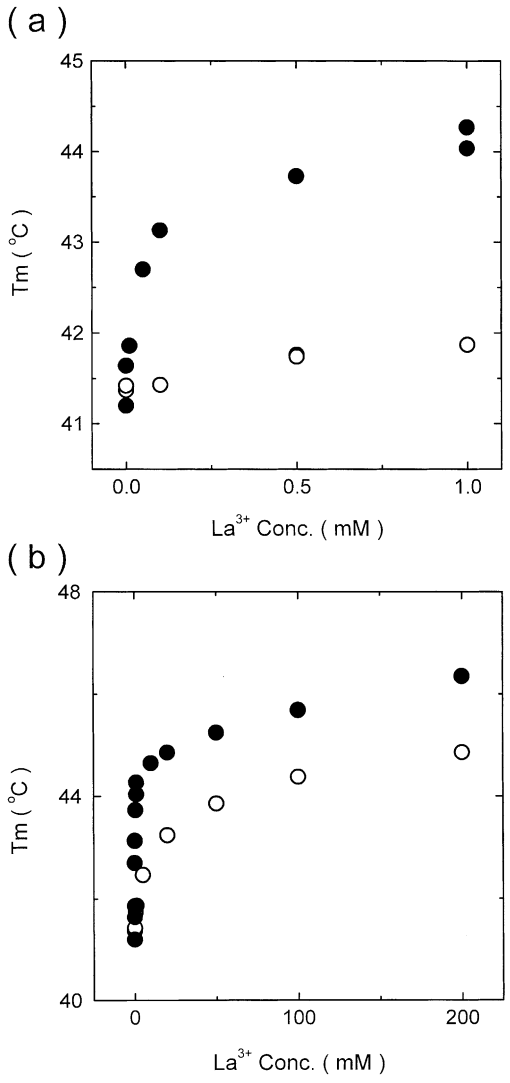

Fig. 6. Dependence of chain-melting temperature of DPPC-MLV on La^{3+} concentration in the absence of KCl and in the presence of 0.5 M KCl. Chain-melting transition temperature of 30 μM DPPC-MLV in the presence of 0 M KCl (○) and 0.5 M KCl (●). (a) 0–1 mM La^{3+} concentration range, and (b) 0–200 mM La^{3+} concentration range. Heating rate was 1.0 °C/min.

3.3. Effect of La^{3+} on spontaneous curvature of DOPC/cholesterol monolayer membrane

To consider the mechanism of the shape changes of DOPC-GUV or DOPC/cholesterol-GUV induced by La^{3+} (or Gd^{3+}), we have investigated the effects of La^{3+} on the spontaneous curvature of DOPC/cholesterol monolayer membrane. To allow the lipid membranes in the hexagonal II (H_{II}) phase to express the spontaneous curvature, H_0, the addition of alkanes such as tetradecane to the membranes is required because they fill the interstitial region of the H_{II} phase and relax the alkyl chain packing stress [31,32]. As reported previously, 60 mol% DOPC/40 mol% cholesterol membrane containing 16 wt.% tetradecane in excess water condition at 20 °C in 10 mM PIPES buffer (pH 7.0) was in

the H_{II} phase [31]. Thereby, to get information on the dependence of the spontaneous curvature of the DOPC/cholesterol membrane on La^{3+} concentration, we have investigated the structure of 60 mol% DOPC/40 mol% cholesterol membrane containing 16 wt.% tetradecane in excess water condition at 20 °C in various concentrations of La^{3+} (Fig. 7a). The basis vector length of the H_{II} phase of the DOPC/cholesterol/tetradecane membrane (center to center distance of adjacent cylinders), d, calculated by $d=(2/\sqrt{3})x$ (x is the spacing in the SAXS) gradually decreased from 12.4 to 10.6 nm with an increase in La^{3+} concentration from 0 to10 mM. In the presence of 0.5 M KCl, the basis vector length, d, of the same DOPC/cholesterol/tetradecane membrane largely decreased with an increase in La^{3+} concentration compared with that in the absence of KCl (Fig. 7b).

We also investigated the effect of La^{3+} on the structure of DOPC membrane containing 16 wt.% tetradecane in excess water condition at 20 °C in 10 mM PIPES buffer (pH 7.0). In the absence of La^{3+} and also in the presence of La^{3+} (from 0 to 100 mM), the membranes were in the L_α phase. The presence of 0.5 M KCl did not change the result; the membranes were in the L_α phase irrespective of La^{3+} concentration (from 0 to 100 mM).

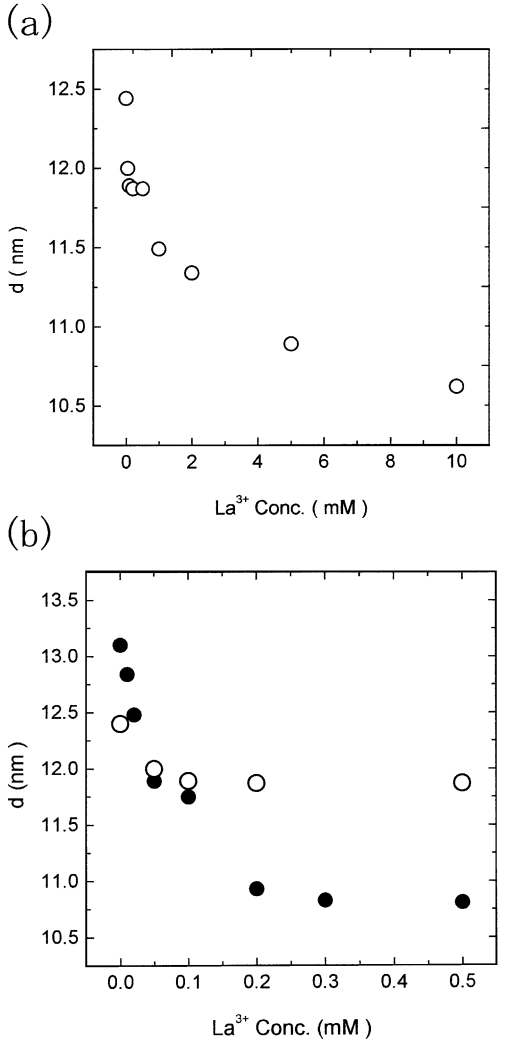

Fig. 7. Basis vector length, d, of the H_{II} phase of the 60 mol% DOPC/40 mol% cholesterol/tetradecane membrane in various La^{3+} concentrations in 10 mM PIPES buffer (pH 7.0) (○) and, d of the same membrane in 10 mM PIPES buffer (pH 7.0) containing 0.5 M KCl (●) at 20 °C. (a) 0–10 mM La^{3+} concentration range, and (b) 0–0.5 mM La^{3+} concentration range.

4. Discussion

4.1. La^{3+} and Gd^{3+} induce several shape changes of DOPC-GUVs

The experimental results clearly indicate that a very low concentration (10 μM) of La^{3+} (or Gd^{3+}) could induce several types of shape changes of the DOPC-GUV. In the observation, we continued to add a given concentration such as 10 μM of La^{3+} (or Gd^{3+}) solution through the micropipette near the GUV for less than 5 min. During the addition of La^{3+} (or Gd^{3+}), the diffusion of La^{3+} (or Gd^{3+}) from the neighborhood of the GUV into the bulk phase occurred. Thereby, we observed these events at the steady state condition of the ion concentration near the GUV, not at the equilibrium condition. The ion concentration near the GUV at the steady state condition is a little lower than that of the solution which was added through the micropipette. Moreover, during the addition of La^{3+} (or Gd^{3+}) for less than 5 min, the equilibrium of binding of the ion on the membrane surface from the neighborhood of the GUV may not be attained. Therefore, we have to keep in mind that in this report, the effects of La^{3+} (or Gd^{3+}) on the shapes of GUVs were observed under this steady state condition for less that 5 min. When we stopped the addition of La^{3+} (or Gd^{3+}), the ions near the GUV were diffused into the bulk phase, and thereby, the ion concentration near the GUV gradually decreased to 0 mM. During this dilution of the ions near the GUV, we observed that the shapes of the GUVs returned to the original ones in water, indicating that at less than critical concentration of La^{3+} (or Gd^{3+}) shapes of GUVs returned to the original ones, and thereby, these shape changes of GUVs were reversible. What kind of effects of these ions on the phospholipid membranes can induce such shape changes of the GUV? La^{3+} (or Gd^{3+}) (10 μM) induces a very low osmotic pressure, and thereby, an effect of the osmotic pressure on the shape of the GUV is negligible. To consider this problem, it is important to analyze the effects of La^{3+} on the physical property of PC membrane. At first, we consider the effect of La^{3+} on phase transition temperatures of DPPC-MLV.

4.2. The mechanism of the increase in phase transition temperatures of DPPC-MLV induced by La^{3+}

We could observe the effect of La^{3+} on the chain-melting temperature (T_m) of the very low concentration (30 μM) of DPPC-MLV for the first time. As shown in Fig. 5, T_m of

DPPC-MLV in water increased with an increase in La^{3+} concentration. This result is consistent with others' data using high concentrations of DPPC-MLV [34,35]. Our results show that the dependence of T_m on La^{3+} concentration was independent of the phospholipid concentration, indicating that T_m was not determined by the molar ratio of DPPC to La^{3+}, but by the La^{3+} concentration only. The larger increase in T_m of DPPC-MLV in the presence of 0.5 M KCl (Fig. 6) indicates that the binding of La^{3+} on the membrane interface is a main cause of the increase in T_m, because the binding of La^{3+} is much enhanced because the electric potential due to the positive surface charges of La^{3+} bound on the membrane surface is largely screened in the presence of a high concentration of salts such as KCl [11]. What kind of factor is important for these phenomena?

In equilibrium, three kinds of lateral pressures in the membrane have to balance, i.e., $\Pi_{head}+\Pi_{chain}=\gamma$, where Π_{head} is the steric repulsive interaction between the head groups in the phospholipid membrane, Π_{chain} is the repulsive chain pressure, and γ is the attractive interfacial pressure due to the hydrophobic interaction between the alkyl chains and water at the membrane interface [36]. The experimental results of the increase in the chain-melting transition temperature, T_m (Figs. 5 and 6) of the DPPC-MLV indicate that the lateral compression pressure of the membrane, $\gamma-\Pi_{head}$, increases with an increase in La^{3+} (or Gd^{3+}) concentration. We can assume that γ is almost constant in the presence of low concentrations of La^{3+} (or Gd^{3+}). Therefore, Π_{head} decreases with an increase in La^{3+} (or Gd^{3+}) concentration. Similar situations where the increase in the lateral compression pressure induces an increase in T_m were observed in other systems [30,37,38]. On the other hand, the binding of La^{3+} (or Gd^{3+}) on the membrane surface of the DPPC-MLV increases the surface charge density, which has an effect of decreasing T_m due to the electrostatic repulsive interaction [39,40]. Therefore, in this case, the effect of the lateral compression pressure on T_m (i.e., the increase in T_m) is a prevailing effect over that of the electrostatic interaction due to the surface charge on T_m (i.e., the decrease in T_m). This is the same situation as the low pH-induced increase in T_m of dihexadecylphosphatidylcholine (DHPC) membrane [38]. In the interaction of La^{3+} on the structure and phase stability of phosphatidylethanolamine (PE) membranes, similar effects were observed [41]. Chain-melting transition temperature of dielaidoyl-PE (DEPE) membrane increased with an increase in La^{3+} concentration, indicating that the lateral compression pressure of the membrane increased with an increase in La^{3+} concentration. This can reasonably explain that La^{3+} can stabilize the H_{II} phase rather than the L_α phase [41].

What is the mechanism of the decrease in the repulsive interaction between the head groups in the phospholipid membrane, Π_{head}, with an increase in La^{3+} (or Gd^{3+}) concentration? Current physical investigations of phospholipid membranes clearly show that their membrane interfaces have dynamic structures and consist of a complex and thermally disordered mixture of hydrophilic segments of the head group, hydrophobic segments of alkyl chains, and water molecules [36,37]. The binding or interaction of substances with the membrane interface largely changes its structure, its surface area, and also intermolecular interactions such as Π_{head} in the membrane interface [32,38]. Hence, in the case of the membrane interface of phospholipid membranes, the change in the surface free energy is not determined only by the adsorption (i.e., the surface excess) of substances on the membrane interface according to the Gibbs surface-tension equation [42]. Therefore, we have to consider the effect of the interaction of substances with the membrane interface on its structure and physical property. Solid NMR method (^{2}H-NMR) revealed that La^{3+} can bind with the head groups of electrical-neutral PC membrane and induce a conformational change of the head group moving the N end of P→N vector of the head groups toward the water phase at relatively high concentrations (5–500 mM), while in the water, in the absence of these ions, the head groups orient almost parallel to the membrane surface, i.e., the P→N vector of the head group is extended almost parallel to the membrane surface [10,11,43]. The degree of the saturation of the binding of La^{3+} in the membrane interface of DPPC membrane in the L_α phase, θ ($=n/n_t$, where n and n_t are the numbers of occupied and total binding sites of the membrane, respectively), is 0.22 at 5 mM La^{3+} [11]. This conformational change decreases Π_{head}. However, ^{2}H-NMR experimental data on the conformation of the head group of PC at less than 1 mM La^{3+} have been never reported. Thereby, at present, we don't have an experimental evidence on the La^{3+}-induced conformational change of the head group at less than 1 mM La^{3+}. La^{3+} may bind with the head group of the PC membrane near the phosphate group, which induces an electrostatic attraction between the negative charges of the phosphate groups (O^-) of neighboring phospholipids. Moreover, this binding may induce a decrease in the number of water molecules near the phosphate group, as reported in the protonation of the phosphate group of PC membrane [38]. Thereby, these may induce a decrease in Π_{head} without the large conformational change of the head group described above. However, further investigation on the interaction of low concentrations (1 μM–1 mM) of La^{3+} with the membrane interface is necessary.

The increase in the lateral compression pressure of the membrane can reasonably explain the decrease or the disappearance of the undulation motion of the GUV membranes in the presence of La^{3+} (or Gd^{3+}). Mathivet et al. [28] have shown a similar phenomenon: the addition of fatty acid-free bovine serum albumin (BSA) into the solution of GUV containing a small amount of lyso-phosphatidylcholine (lyso-PC) inhibited the undulations of the membrane of GUV, because BSA selectively depletes the lyso-PC in the external membranes, inducing an increase in the lateral compression pressure in the membrane. Their results support the above analysis.

4.3. The effect of La^{3+} on the spontaneous curvature of DOPC/cholesterol monolayer membrane

The increase in the lateral compression pressure of the membrane induced by La^{3+} induces a decrease in the surface area of the membrane. However, it is difficult to measure a small change of the surface area of lipid membranes less than 1% by SAXS [44] and micropipette aspiration method [13,45]. Here, we could detect indirectly the decrease in the surface area per lipid molecule of the DOPC/cholesterol membrane by the measurement of the spontaneous curvature. The result of Fig. 7 gives information on the change of the radius of spontaneous curvature R_o of the 60 mol% DOPC/40 mol% cholesterol monolayer membrane. The basis vector length of the H_{II} phase, d, is expressed as a sum of the radius of water tube, R_w, and the thickness of the monolayer membrane, d_l, i.e., $d=2\ (R_w+d_l)$ [32]. In excess water, the DOPC/cholesterol membrane containing 16 wt.% tetradecane in the H_{II} phase has a curvature close to $H_0\ (=1/R_o)$ to minimize the curvature free energy, and thereby, $R_w \approx R_o$ [31]. The decrease in d of the DOPC/cholesterol/tetradecane membrane induced by La^{3+} is attributed to the decrease in R_w, since the change in d_l is assumed to be small. Thus, the result of Fig. 7 indicates that R_o of the DOPC/cholesterol membrane decreased with an increase in La^{3+} concentration. The larger decrease in d, which means the larger decrease in R_o of the DOPC/cholesterol membrane in the presence of 0.5 M KCl indicates that the binding of La^{3+} on the membrane is the main cause of the decrease in R_o. On the other hand, H_0 can be expressed in terms of the packing parameter (V/al) of the phospholipid molecule, where V is the average volume of the entire lipid molecule, l is its average length, and a is the average area of the lipid head group at the lipid–water interface, and that in the inverted curved structures, absolute values of H_0 increases (i.e., R_o decreases) with an increase in V/al [46]. Thereby, the packing parameter (V/al) of the DOPC/cholesterol membrane increases with an increase in La^{3+} concentration, indicating that the area of the lipid head group, a, decreases with an increase in La^{3+} concentration since V and l are almost constant. However, at present, we don't have any direct experimental evidence for the effect of La^{3+} on the area of the DOPC membrane.

4.4. The mechanism of the shape change of DOPC-GUV induced by La^{3+} or Gd^{3+}

As discussed in the previous sections, La^{3+} or Gd^{3+} induces the increase in the lateral compression pressure of the PC membranes, which induces a decrease in the surface area of the membrane. In the experiments of the shape change of GUVs, La^{3+} (or Gd^{3+}) was added into the neighborhood of GUVs from the outside of the GUVs. Moreover, these ions cannot pass through the bilayer membranes of the GUVs, and thereby, don't exist inside the GUVs. Therefore, only the area of the external monolayer membrane of the DOPC-GUV, A^{ex}, decreases due to the interaction of La^{3+} (or Gd^{3+}) with the external monolayer membrane, while the area of the internal monolayer, A^{in}, does not change. Hence, the interaction of La^{3+} (or Gd^{3+}) with the GUV induces a decrease in the area difference between the two monolayers in the bilayer membrane, $\Delta A\ (=A^{ex}-A^{in})$, without the change of the volume of the GUV. On the other hand, the analysis based on the bilayer-couple model [23,24] shows that, under the condition of the constant volume of the GUV, the shape transformations such as the discocyte to stomatocyte to inside budded shape and the two-spheres connected by a neck to prolate transformation [23,24] and also the pearl on a string to cylinder transformation [47] occur with a decrease in ΔA. The ADE model also predicts a similar shape change [26,27]. Therefore, the several types of shape changes of the DOPC-GUV induced by La^{3+} (or Gd^{3+}) can be explained reasonably by the decrease in ΔA. To prove our model for the mechanism of the shape change of the DOPC-GUV, we need more experiments and quantitative analysis in the future.

5. Conclusion

We have found that a very low concentration (10 μM) of La^{3+} (or Gd^{3+}) induced a shape change of DOPC-GUV such as the discocyte via stomatocyte to inside budded shape transformation, the two-spheres connected by a neck to prolate transformation, and the pearl on a string to cylinder transformation. These ions also increase the chain-melting phase transition temperature and the $L_{\beta'}$ to $P_{\beta'}$ phase transition temperature of DPPC-MLV, which can be explained by the increase in the lateral compression pressure of the membrane induced by the binding of these ions on the membrane interface. Thereby, the interaction of La^{3+} (or Gd^{3+}) on the external monolayer membranes of the GUV induces the decrease in its area, and hence, ΔA decreases. The shape changes of the DOPC-GUV induced by La^{3+} (or Gd^{3+}) are consistent with the simulation results when ΔA decreases based on the bilayer-couple model and also the ADE model. The increase in the lateral compression pressure of the membrane induced by these ions may play an important role in the effects of these ions on the stability and functions of membrane proteins such as ionic channel [41].

Acknowledgements

This research was supported partly by a grant from the Asahi Glass Foundation to M.Y.

References

[1] M. Gustin, X.-L. Zhou, B. Martinac, C. Kung, Science 242 (1988) 762–765.
[2] X.-C. Yang, F. Sachs, Science 243 (1989) 1068–1071.
[3] X.-L. Zhou, C. Kung, EMBO J. 11 (1992) 2869–2875.

[4] J. Lee, A. Ishihama, G. Oxford, B. Johnson, K. Jacobson, Nature 400 (1999) 382–386.
[5] M. Takata, W.F. Pickard, J.Y. Lettvin, J.W. Moore, J. Gen. Physiol. 50 (1966) 461–471.
[6] C.M. Armstrong, G. Cota, J. Gen. Physiol. 96 (1990) 1129–1140.
[7] M.M. Hammoudah, S. Nir, T. Isac, R. Kornhauser, T.P. Stewart, S.W. Hui, W.L.C. Vaz, Biochim. Biophys. Acta 558 (1979) 338–343.
[8] J. Bentz, D. Alford, J. Cohen, N. Düzgünes, Biophys. J. 53 (1988) 593–607.
[9] M. Petersheim, J. Sun, Biophys. J. 55 (1989) 631–636.
[10] M.F. Brown, J. Seelig, Nature 269 (1977) 721–723.
[11] H. Akutsu, J. Seelig, Biochemistry 20 (1981) 7366–7373.
[12] J. Seelig, P.M. Macdonald, P.G. Scherer, Biochemistry 26 (1987) 7535–7541.
[13] R. Kwok, E. Evans, Biophys. J. 35 (1981) 637–652.
[14] E. Evans, W. Rawicz, Phys. Rev. Lett. 64 (1990) 2094–2097.
[15] W. Rawicz, K.C. Olbrich, T. McIntosh, D. Needham, E. Evans, Biophys. J. 79 (2000) 328–339.
[16] H. Hotani, J. Mol. Biol. 178 (1984) 113–120.
[17] K. Berndl, J. Käs, R. Lipowsky, E. Sackmann, U. Seifert, Europhys. Lett. 13 (1990) 659–664.
[18] J. Käs, E. Sackmann, Biophys. J. 60 (1991) 825–844.
[19] E. Farge, P.F. Devaux, Biophys. J. 61 (1992) 347–357.
[20] A. Saitoh, K. Takiguchi, Y. Tanaka, H. Hotani, Proc. Natl. Acad. Sci. U. S. A. 95 (1998) 1026–1031.
[21] Y. Yamashita, M. Oka, T. Tanaka, M. Yamazaki, Biochim. Biophys. Acta 1561 (2002) 129–134.
[22] H.J. Deuling, W. Helflich, J. Phys. 37 (1976) 1335–1345.
[23] S. Svetina, B. Zeks, Eur. Biophys. J. 17 (1989) 101–111.
[24] U. Seifert, K. Berndl, R. Lipowsky, Phys. Rev. A 44 (1991) 1182–1202.
[25] B. Bozic, S. Svetina, B. Zecks, R.E. Waugh, Biophys. J. 61 (1992) 963–973.
[26] W. Wiese, W. Harbich, W. Helfrich, J. Phys.: Condens. Matter 4 (1992) 1647–1657.
[27] L. Miao, U. Seifert, M. Wortis, H.-G. Döbereiner, Phys. Rev. E 49 (1994) 5389–5407.
[28] L. Mathivet, S. Cribier, P.F. Devaux, Biophys. J. 70 (1996) 1112–1121.
[29] G.R. Bartlett, J. Biol. Chem. 234 (1969) 466–468.
[30] M. Yamazaki, M. Ohshika, N. Kashiwagi, T. Asano, Biophys. Chem. 43 (1992) 29–37.
[31] Z. Chen, R.P. Rand, Biophys. J. 73 (1997) 267–276.
[32] K. Kinoshita, S.J. Li, M. Yamazaki, Eur. Biophys. J. 30 (2001) 207–220.
[33] E. Sackmann, in: Structure and Dynamics of Membranes, R. Lipowsky, E. Sackmann (Eds.) Elsevier/North-Holland, Amsterdam, 1995, pp. 213–304.
[34] B.Z. Chowdhry, G. Lipka, A.W. Dalziel, J.M. Sturtevant, Biophys. J. 45 (1984) 633–635.
[35] X.-M. Li, Y.-F. Zhang, J.-Z. Ni, J.-W. Chen, F. Hwang, J. Inorg. Biochem. 53 (1994) 139–149.
[36] J.N. Israelachvili, Intermolecular and Surface Forces, 2nd edn., Academic Press, New York, 1992.
[37] K. Kinoshita, S. Furuike, M. Yamazaki, Biophys. Chem. 74 (1998) 237–249.
[38] S. Furuike, V.G. Levadny, S.J. Li, M. Yamazaki, Biophys. J. 77 (1999) 2015–2023.
[39] H. Träuble, M. Teubner, P. Wooley, H. Eibl, Biophys. Chem. 4 (1976) 319–342.
[40] F. Jähnig, K. Harlos, H. Vogel, H. Eible, Biochemistry 18 (1979) 1459–1468.
[41] T. Tanaka, S.J. Li, K. Kinoshita, M. Yamazaki, Biochim. Biophys. Acta 1515 (2001) 189–201.
[42] R. Lipowsky, H.-G. Döbereiner, Europhys. Lett. 43 (1998) 219–225.
[43] H. Akutsu, T. Nagamori, Biochemistry 30 (1991) 4510–4516.
[44] V. Luzzati, F. Husson, J. Cell Biol. 12 (1962) 207–219.
[45] D. Needham, in: E.A. Disalvo, S.A. Simon (Eds.), Permeability and Stability of Lipid Bilayers, CRC Press, Boca Raton, FL, 1995, pp. 49–76.
[46] D. Marsh, Biophys. J. 70 (1996) 2248–2255.
[47] A. Iglic, V. Kralj-Iglic, J. Majhenc, J. Biomech. 32 (1999) 1343–1347.